ELSEVIER

Tectonophysics 342 (2001) 113–136

TECTONOPHYSICS

www.elsevier.com/locate/tecto

A thermomechanical model of exhumation of high pressure (HP) and ultra-high pressure (UHP) metamorphic rocks in Alpine-type collision belts

E. Burov [a], L. Jolivet [a,*], L. Le Pourhiet [a], A. Poliakov [b]

[a] *Lab Teconique ESA 7072, University of Pierre and Marie Curie, Case 129, T 26-E1, 4, place Jussieu, 75252 Paris Cedex 05, France*
[b] *University of Montpellier II/CNRS, Montpellier, France*

Received 19 July 2000; accepted 3 December 2000

Abstract

Using a fully coupled numerical thermomechanical model handling strain localization, surface processes and ultra-high viscosity contrasts (11 orders of magnitude) we test a number of possible mechanisms of High Pressure (HP)–Low Temperature (LT)/High Temperature (HT) exhumation in continental collision zones. The model considers two end-member cases, low or high buoyancy of the downgoing crust. The first model case predicts three levels of exhumation in the same collisional context: the "classical" corner flow LP–LT (Low Pressure–Low Temperature) exhumation in the accretionary prism; deeper (70 km) HP–HT exhumation for the thickened subducting crustal–sedimentary wedge, and ultra HP–HT exhumation from the "lower" crustal chamber, forming at the depth of 100–120 km and separated from the upper one by a narrow crustal channel. The width of this channel can oscillate in the process of shortening, thus controlling the quantity of the crustal material exchanged between the crustal wedge and the lower crustal chamber. Although both zones of crustal accumulation and the narrow channel between them resemble a vortex-shaped nozzle, this "nozzle" appears to be too soft to produce any significant overpressures. From the upper crustal wedge, the material is exhumed following the ascending shear flow created by the overriding plate assisted by positive buoyancy of the heated crustal material. From the lower crustal chamber, the material is transported upward to the upper crustal wedge by a flow induced by the asthenospheric traction and a small-scale convective instability forming in the lower crustal chamber due to its heating by the overriding asthenosphere. In the second modelled case of high buoyancy, the latter mechanisms become dominant resulting in hyper fast exhumation of the crust to the surface, accelerated or slowed subduction in case of full or partial crustal decoupling, respectively, and upper plate extension.

Keywords: Exhumation; Alpine-type collision; Rheology

1. Introduction

Physical mechanisms of High Pressure–Low Temperature (HP–LT) rock exhumation still stay enigmatic. Most of the known cases of exhumation of HP–LT rocks are associated with continental collision. Specifically for this reason, the most advanced recent models almost always consider compression and/or subduction. Among these models one should mention those of "corner flow and valve effect" (Mancktelow, 1995; Platt, 1993; Shreve and Cloos, 1986) whose authors try to explain the HP–LT exhumation by a circular flow of sedimentary material (containing metamorphic inclu-

* Corresponding author. Fax: +33-1-4427-5085.
E-mail address: laurent.jovilet@lgs.jussieu.fr (L. Jolivet).

0040-1951/01/$ - see front matter
PII: S0040-1951(01)00158-5

sions) in a large accretion prism. Yet these mostly semi-analytical models can be applied only to small up to average depths of about 30–40 km, for accretionary prisms deeper than that are not observed. On the other hand, these models are also too simplistic to reproduce complete $P–T–t$ or even $P–T$ paths. Consequently, a more rigorous numerical approach is needed to tackle the problem in more details as well as to validate the existing conceptual models.

Regarding the exhumation of HP rocks uplifted from depths corresponding to lithostatic pressures of 60–150 km, there is only a couple of models, one of which considers deep subduction of the continental crust (Beukel, 1992; Molnar and Gray, 1979) to the depths of 200–250 km (Chemenda et al., 1995), followed by decoupling and positive buoyancy-driven exhumation of the crustal material from about 100 km (Chemenda et al., 1995, 1996, 1997; Dobretsov, 1991; Ernst and Liou, 1995; Malavieille and Chemenda, 1997). This model has been considered in various mountain belts (Brown et al., 1998; Franke, 1998; Matte, 1998). Yet, like most previous models, it does not handle thermal evolution, which is not only crucial for reproducing $P–T$ paths but also for verification of the rheological possibility of this handy mantle–crust decoupling at the proper moment, and because rheology and buoyancy forces are strongly dependent on temperature. The models of the second type (Cloetingh et al., 1999; Burg and Podladchikov, 1999) explore both the subduction and large-scale compressive instabilities, for example mega-folding, which can be "downwarp" (Cloetingh et al., 1999), or "upwarp" (Burg and Podladchikov, 1999). The large compressive instability is known to be the fastest way to induce vertical surface and subsurface undulations in the lithosphere (e.g., Burov et al., 1993). Since the continental lithosphere is gravitationally unstable, the growth of the compressive mega-folds can be probably accelerated by a Raleigh–Taylor instability (Cloetingh et al., 1999). Folding can transport surface rocks to the depth of 200 km, which can be followed by a compressive upward squeezing of these rocks later resulting in their ultra-rapid uplift (1–15 cm/year) back to the surface.

In this study, we attempt to evaluate the relative role of the possible exhumation mechanisms using direct 2D numerical modeling. Our approach is based on the implicit numerical FLAC-type (Cundall, 1989) algorithm PARAVOZ, (Poliakov et al., 1993; Burov et al., 1998) allowing for high complexity of internal structures, rheologies and thermal conditions. This algorithm is well adapted to lithospheric-scale problems, for it takes into account: (1) brittle–elasto–ductile rheological laws in their generic form, (2) changes in physical properties (density, thermal conductivity, etc.), (3) surface processes (erosion), (4) heat transfer and production; (5) strain-localization (non-predefined faulting, shear bands). Based on this method, we would like to answer a number of fundamental questions such as: (1) Why the exhumation rate can be 5–10 times more important than the tectonic shortening rate? (2) Does the complete pressure value P estimated from petrologic data correspond to a "true" hydrostatic pressure (function of the depth) or can this pressure include an important tectonic component (as suggested in Mancktelow, 1995 or in Petrini and Podladchikov, 2000)? (3) Does the temperature T (600–700 °C) derived from the petrology data for HP–LT rocks correspond to a "normal" geotherm or is it strongly perturbed by the thrusting or flow?

1.1. Exhumation of HP and UHP rocks, a brief review

A large part of the literature devoted to exhumation of HP and UHP rocks has been focussed for the last 10 years or more on two different aspects: (1) the respective contributions of extension and erosion to the removal of the overburden and (2) lithospheric scale processes which may explain the exhumation of UHP metamorphic rocks.

After Platt (1986), who suggested that extension is accommodated along shallow-dipping detachments in the upper parts of accretionary complexes, many examples of such behavior have been proposed in the Alps (e.g., Ballèvre and Merle, 1993; Ballèvre et al., 1990; Bousquet et al., 1998; Selverstone, 1988; Goffé and Chopin, 1986), in the Cyclades and Crete (Jolivet and Patriat, 1999; Jolivet et al., 1996). Syn-orogenic and post-orogenic extension are attested in numerous natural examples and contribute to the removal of significant parts of the crust overlying metamorphic rocks. Whatever is the precise geometry used in conceptual models, either a Coulomb-prism (Platt, 1986) or a migrating accretionary complex (Jolivet et al., 1994, 1999), extension never reaches deep levels of the nappe pile and can be regarded as

an efficient way to remove the overburden, almost like erosion. Only few models consider that intra-crustal detachments may reach the deepest parts of the exhumed crust. One can just refer to the exhumation of coesite-bearing units in the Norwegian Caledonides (Andersen, 1998; Dewey et al., 1993). In most cases extension and erosion cannot be considered as efficient mechanisms for exhumation of UHP rocks from mantle depths. Another major problem relates to that extension is often efficient enough to rework earlier pre-existing structures, especially in rocks that have followed the longest path at depth. One thus has to rely on different approaches to discuss the deep evolution of UHP rocks. $P–T–t$ paths are the best constraints we have at our disposal to test analog or numerical models of orogenic processes.

Most of HP units have never experienced pressures higher than 15–18 kbar and stayed in the domain of formation of blueschists and low-pressure eclogites. These conditions can be obtained within an accretionary complex. Several models have explored the dynamics of such thick prisms (Bousquet et al., 1997; Henry et al., 1997; Le Pichon et al., 1997; Shi and Wang, 1987). Within many HP units, there are also minor UHP components that have experienced much higher pressures revealed by detectable coesite-or diamond-bearing parageneses (Chopin, 1984; Chopin et al., 1991; Smith, 1984; Wain, 1997). The original rocks were formed either at the surface (metasediments in the Alps) or in the deep crust (eclogitized granulites of Caledonides). We are thus facing a very deep material circulation, which cannot be explained in terms of a simple accretionary complex. To attain pressures on the order of those expected in the mantle, rocks must be driven along the subduction plane to depths as deep as 100–150 km, of course if one assumes no significant tectonic overpressure. It is evident that the possibility of important tectonic overpressure cannot be precluded. Nevertheless, most of the existing overpressure models face a number of difficulties in confrontation with the data. One of the most commonly inferred conceptual overpressure models is Mancktelow's (1995) channel flow model. This analytical model assumes that the flow of the sedimentary/crustal material in a narrow valve-shaped channel between the subducting and overriding plates can produce dynamic overpressures twice higher than the lithostatic pressure at 20–40 km depth. Yet, this model does not explain a number of phenomena such as volatile recycling and does account for thermal evolution. It is also based on several important assumptions such as that of a constant material influx and of a rigid canal geometry. The latter condition might be difficult to handle in the real lithosphere, because the predicted tectonic overpressure (hundreds of MPa) is close to or exceeds the yield strength of the lithosphere. It is thus more realistic to assume that the subduction channel will rather widen or break instead of maintaining high overpressures. The overpressure model by Petrini and Podladchikov (2000) suggests stability of mountains requires compressive tectonic stresses as high as the lithostatic pressure, which would double the total pressure in the collision belts. This model considers the lithosphere as a continuous horizontal ductile channel (lower crust) delimited by flexible rigid upper and lower walls (upper crust and mantle lithosphere, respectively). It assumes that the material cannot escape through the bounding competent layers and that the deformation cannot be localized in a specific area, contrary to what actually happens in most collision zones.

According to the geo-petrological data (e.g., Agard et al., 1999), the formation and exhumation of HP and UHP metamorphic complexes seems to follow at least two different circuits:

1. A quite shallow circulation within accretionary complexes that accounts for the formation and exhumation of blueschists and most eclogites;
2. A deeper (high pressure) circulation, which is responsible for the formation and exhumation of UHP eclogites.

It is not clear how much these two levels of circulation are connected because outcropping rocks show a multitude of pressure values that are distributed in the interval between the greenschists and UHP eclogites without any significant gap. The example of the Schistes Lustrés nappe is a quite representative case of a regular increase of metamorphic pressure across a methamorphic belt from non-metamorphosed sediments at the front to UHP metasediments in the Dora Maira massif (Agard et al., 1999). We exclude the case of significant non-lithostatic pressures, because in this case the maximum depth might not be very large. If no important tectonic overpressure is present, then the

forces, which control deep circulation, are either imposed by the geometry of the model or by contrasts of density between HP rocks and their environment. The classical corner-flow model (Shreve and Cloos, 1986) is controlled by the triangular geometry of the accretionary complex. In this model, the deeper rocks are exhumed to the surface because of underthrusting by new material, which is dragged below them. It is theoretically possible to exhume small blocks of dense material embedded within a lighter matrix and several such models have been proposed (calcareous, muddy or serpentinite matrix (Maekawa et al., 1993, 1995)). When large bodies of UHP rocks such as the Western Gneiss Region in the Norwegian Caledonides are exhumed, the problem becomes more difficult to solve. It has been shown that once basic or intermediate rocks have been equilibrated in the eclogite facies, they can easily reach densities higher than that of the mantle (Austrheim and Boundy, 1994; Austrheim et al., 1997; Bousquet et al., 1997). There is thus a physical problem to exhume such rocks to the surface, since there will be no positive driving buoyancy forces and consequently supplementary forces will be required. Several studies used this hypothetical strong density increase as argument in favor of a decoupling between the upper and lower crust during subduction and of almost complete disappearance of the lower crust in most mountain belts (Dewey et al., 1993; Jolivet et al., 1999; Le Pichon et al., 1997). However, since it is not granted to assess the percentage of recrystallization during metamorphism, it is also difficult to estimate the effective density of the deeply subducted crust in each particular case. One can reasonably assume that fluid-rich protoliths such as metapelites will be fully equilibrated within a short time interval, but the case of basic rocks and lower crustal granulites appears to be much more problematic. Field examples show that large bodies of metastable parageneses remain within the Western Gneiss region although the whole domain experienced eclogite $P–T$ conditions (Andersen and Jamtveit, 1990; Andersen et al., 1994; Austrheim and Boundy, 1994; Boundy et al., 1997; Engvik and Andersen, 2000; Engvik et al., 2000). It is thus difficult to precisely constrain the evolution of the average density at depth during convergence, and for this reason we leave this important part of the problem for further development. The preliminary approach described in this paper will not explore possible peculiarities of phase changes during deformation, but will merely consider two end-member cases: full metamorphism (at 700 °C all subducted crustal material becomes of the same density as the mantle) and weak metamorphism (no density changes due to metamorphism).

2. Model and results

The geodynamic sketch shown in Fig. 1 presents an Alpine-like collision model setup. In this two-dimensional model, the colliding lithospheric plates are composed of different lithological layers, which geometry is derived from the European geotraverse and ECORS data (e.g., Burov et al., 1999) (Fig. 1). In many aspects the problem geometry is analogous to that used in Bousquet et al. (1997). The principal difference is in physical and numerical approach used. Bousquet et al. (1997) proposed a kinematic thermal model, in which they imposed the kinematics of subduction and arbitrarily chosen the depth of decoupling either at the base of the sedimentary column or between the upper and lower crusts. This kinematic model was used to solve heat transfer equations assuming that densities evolve with P and T according to a predefined $P–T$ table. We used a fully coupled large strain thermo-mechanical model, which accounts for force and stress balance, material and energy conservation (including heat transfer), realistic elasto–plasto–ductile rheology and surface processes. Imposed are only the initial geometry, temperature distribution and physical properties. We use two different geometries for the plate contact. The first involves a backstop dipping opposite to the subducting plate. The second one imposes a backstop dipping inland toward the upper plate. The geometry of the accretionary prism near the surface is thus drastically different in these cases. The lateral boundary conditions are imposed as convergence rates, at top free surface boundary condition is used, the bottom surface is supported by a pliable Winkler basement (Fig. 1). Rates of convergence vary between 3 and 6 mm/year in agreement with the estimations made by Schmid et al. (1997).

The numerical finite element code PARAVOZ used in this study allows for direct implementation of various possible collision scenarios. We can, for example, directly introduce the deep lithological and

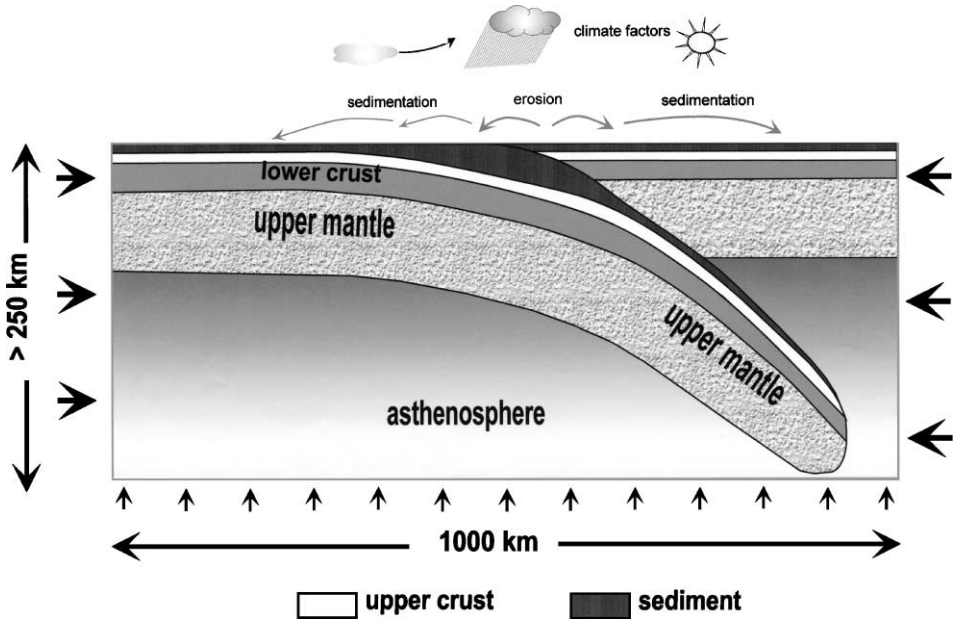

Fig. 1. Problem setup: Alpine collision-like continental subduction scheme derived from the European geotraverse and ECORS data. The model takes into account the lithological and rheological structure, surface processes and uses shortening rate as lateral boundary condition.

rheological structures derived from seismic and gravity profiles, thermal and rock mechanics data, and use known horizontal convergence rates as the boundary conditions. PARAVOZ is a hybrid finite-element/differences fully explicit time-marching Lagrangian algorithm derived from the FLAC algorithm (see Cundall, 1989 for details). The PARAVOZ algorithm and its geophysical implementations were described in detail in a number of recent publications (Poliakov et al., 1993; Burov and Molnar, 1998; Burov and Poliakov, 2001; Burov et al., 1999; Cloetingh et al., 1999). For this reason, we limit the description of the code to a very short outline of its major features.

2.1. The equations solved

The code solves the Newton equation of motion in continuum mechanics formulation coupled with heat transport equation:

$$\rho\partial v_i/\partial t - \partial\sigma_{ij}/\partial x_j - \rho g_i = 0. \quad (1)$$

$$\mathrm{div}(\mathbf{k}\nabla T) - \rho C_\mathrm{p}\partial T/\partial t + H_\mathrm{r} = \mathbf{v}\nabla T.$$

where v and $\mathbf{v}$ are the velocity and velocity tensor, respectively, g is the acceleration due to gravity and ρ is the density. C_p is the specific heat, $\mathbf{k}$ is the thermal conductivity tensor, H is the radiogenic heat production per unit volume (here, we use the commonly adopted inferred values, e.g., in Burov et al., 1993).

The method allows us to use small strain formulation for large strain problems because the Lagrangian numerical mesh moves with the material, and at each time step the new positions of the mesh grid nodes are calculated from the current velocity field and updated in large strain mode accounting for stress rotation. Solution for velocities at mesh points is used to calculate element strain components ε_{ij}. These strains are employed in the constitutive relations yielding element stresses σ_{ij} and equivalent forces $\rho\partial v_i/\partial t$, which provide input for the next calculation cycle. Solutions on the right-hand side (diffusion) and left-hand side (advection) of the heat transfer equation are separated: the latter is calculated automatically when solving the equations of motion, whereas the former is computed using a separate procedure.

In this code, we additionally incorporated: (a) erosion/sedimentation model employed in Burov and Cloetingh (1997); (b) rheological and lithological model similar to that of Burov and Cloetingh (1997); (c) heat advection and diffusion processes;

(d) initial temperature field for continental lithosphere (Burov and Diament, 1995). PARAVOZ can handle rheologically complex behaviors in large strain mode, including localization and propagation of non-predefined faults (shear bands), power law creep and various kinds of strain softening and work hardening behaviors (for geodynamic applications see Burov and Guillou-Frottier, 1999; Burov and Molnar, 1998; Gerbault et al., 1998, 1999).

2.2. Rheology and physical properties of the rocks

Brittle–elasto–ductile non-linear rheology is assumed for all materials. The crust and sediment (which initially fills the uppermost part of the foreland basin and also created by erosion) are presented by a quartz-dominated lithology. The mantle is presented by olivine-dominated lithology. We used commonly inferred rheological parameters: the elastic moduli, ductile creep material constants, activation energies and power exponents adopted here come from Burov et al. (1999) (see also Section 3.2.3). The brittle part is approximated by Mohr–Coulomb plasticity with 30° friction angle and 20-MPa cohesion for all materials except sediments, which have smaller cohesion of 5 MPa. The densities are 2300, 2650, 2800, 3330 and 3250 kg/m^3 for the sediment, upper crust, lower crust, mantle and asthenosphere, respectively. The thermal conductivities are: 1.6, 2.5, 2, 3.5, 3.5 W m^{-1} °K^{-1} for the sediment, upper crust, lower crust, mantle and asthenosphere, respectively. The thermal expansion coefficient used is 3.1×10^{-5} °K^{-1}.

2.3. Surface processes

It was shown in a number of studies (e.g., Métivier and Gaudemer, 1997; Avouac and Burov, 1996) that surface processes have to be incorporated in continental orogeny models because the erosion rates in active collision zones are of the same order as the vertical tectonic rates, and also because erosion is one of the major processes responsible for surface exposure of the exhumed material.

Following Avouac and Burov (1996), we used linear diffusion erosion for the short-range surface processes (coefficient of erosion is scale-depended and varied from 0 to 8000 m^2 year^{-1}) and flat deposition outside the elevated topography range. The values of the erosion parameters are largely scale-dependent. For this reason, they were experimentally adopted to keep the topography growth rates and the resulting erosion and sedimentary rates within geologically reasonable limits.

2.4. Deep phase transitions

The adopted numerical algorithm allows for various kinds of phase transitions. For example, surface phase transitions are implemented in the erosion subroutine, which converts basement rock into sedimentary matter with appropriate changes in density, thermal and mechanical properties. However, we introduced only simplified deep phase changes, because the percentage and character of eclogitization are too much uncertain. We thus decided to consider two end-member situations: low-buoyancy and high-buoyancy phase changes. In the first case, all subducting crust turns to a heavy material of the same density as that of the mantle. In this case, it is only thermal expansion that makes metamorphed crustal parts slightly lighter than the mantle parts, which is sufficient to drive some gravity instability (see below). In the second case, the density of the crust does not change. These two end-member cases can be understood as two opposite scenarios corresponding to a maximum and minimum degree of eclogitization.

As discussed above, it is difficult to assess the exact composition of the subducted lower crust and quantify how much of it is basic. It even more difficult to determine how much of the basic rocks are fully recrystallized to eclogites during the burial process, not mention that the final eclogites may have quite different densities, dependent on the alkalinity and fluid content. Consequently, in the low-buoyancy case, we simply assume a high ratio of eclogitization, and in the high-buoyancy case we suppose that eclogitization is not significant at the scale of the crust or that the crust is not basic enough for a significant effective density increase to occur.

3. Experiments

We conducted a set of experiments employing a representative Alpine-like collision scenario, which was tested against major possible combinations of

weak and strong rheological layers in the lithosphere. We used the same set of rheological and thermal parameters as in Burov et al. (1993, 1999) assuming brittle–elasto–ductile lithosphere composed of quartz-rich upper and lower crust and olivine controlled mantle. An initial thermal structure was imposed using a conventional thermal distribution for a specified thermotectonic age (Burov and Diament, 1995). The exceptional feature of the approach implemented here is a very high viscosity contrast (up to 11 orders of magnitude) maintained in some of the experiments, allowing us to handle short-term processes such as convective instabilities in the reheated subducted crust.

3.1. Low-buoyancy mechanisms

The experiment shown in Figs. 2 and 3 demonstrates the consecutive stages of continental subduction occurring within 50-m.y. time interval at "Alpine" shortening rate of 3 mm/year and assuming "full eclogitization" (high density 3330 kg/m^3) of the entire downgoing crust.

3.1.1. Plastic hinging of the slab

One can see that after the first 10 m.y., the initially narrow channel between the subducting and overriding plate significantly change its geometry towards vortex nozzle shapes. This geometry resembles that predicted in a number of studies (e.g., Mancktelow, 1995), but the physical mechanism behind it is absolutely different from any of the previously proposed ones. The lower crustal chamber forming below the "valve" neck is a result of localized ductile yielding in the mantle lithosphere caused by flexural stress. This effect, known as plastic hinging, takes place in strongly bent inelastic layers, of which flexure of elasto–brittle–ductile lithosphere is a good example (Burov and Diament, 1995, 1996). Bending results in strain concentration at the inflection points. When the flexural stress exceeds strength limits at inflection point, the material yields locally, resulting in localized necking of the competent portion of the bent layer and formation of weak ductile or brittle zones above and below it. Any further bending concentrates in the weakened zone, which becomes less and less resistant and finally starts to act as a hinge. Progressive bending results in progressive localized thinning of the competent core and in proportional enlargement of the adjacent weak inelastic zones. This effect explains strong thinning of competent mantle in the area of utmost lithospheric bending. The weakened ductile zone above the competent mantle core can be eroded and filled with ductile crustal material.

3.1.2. Formation of a backthrust

Fig. 2a shows early formation of a backthrust in the convergence process. The stable configuration thus seems closer to the one with a backstop dipping toward the trench, chosen in the experiment from Figs. 2 and 3. The formation of the non-predefined backthrust is an important result allowing for validation of the model. The development of the backthrust is conditioned by the effective resistance of the crust of the overriding plate, which is controlled by rheological composition, temperature and deformation rate. In general, we noticed that the backthrust does not form if the crustal strength of the upper plate is very low. Yet, the problem of backthrust formation is beyond the scope of the present study and should be left for further investigations. Backthrusting apparently does not change the general exhumation pattern predicted for the low-buoyancy case.

3.1.3. No tectonic overpressures

Contrary to the prediction of the Mancktelow (1995) model, there is no remarkable overpressure in the crustal "valve" neck. The Manktelow model assumes a fixed valve geometry, like that of a jet engine nozzle, but the numerical experiment shows that the channel tends to widen itself in response to any slight increase in pressure. Thus, non-lithostatic pressure in any parts of the nozzle does not exceed 20–40 MPa. Our study thus dismisses most previously proposed tectonic overpressure models based on nozzle–valve effect. Of course, this result does not exclude other possible mechanisms for tectonic overpressure.

3.1.4. Topography and slab break-off

A maximum topography is reached after 20 m.y. of convergence and the mountain belt starts to broaden once the increasing body forces start to counterbalance boundary forces. After 50 m.y. the mountain belt totally collapsed, as could be expected in case of slab

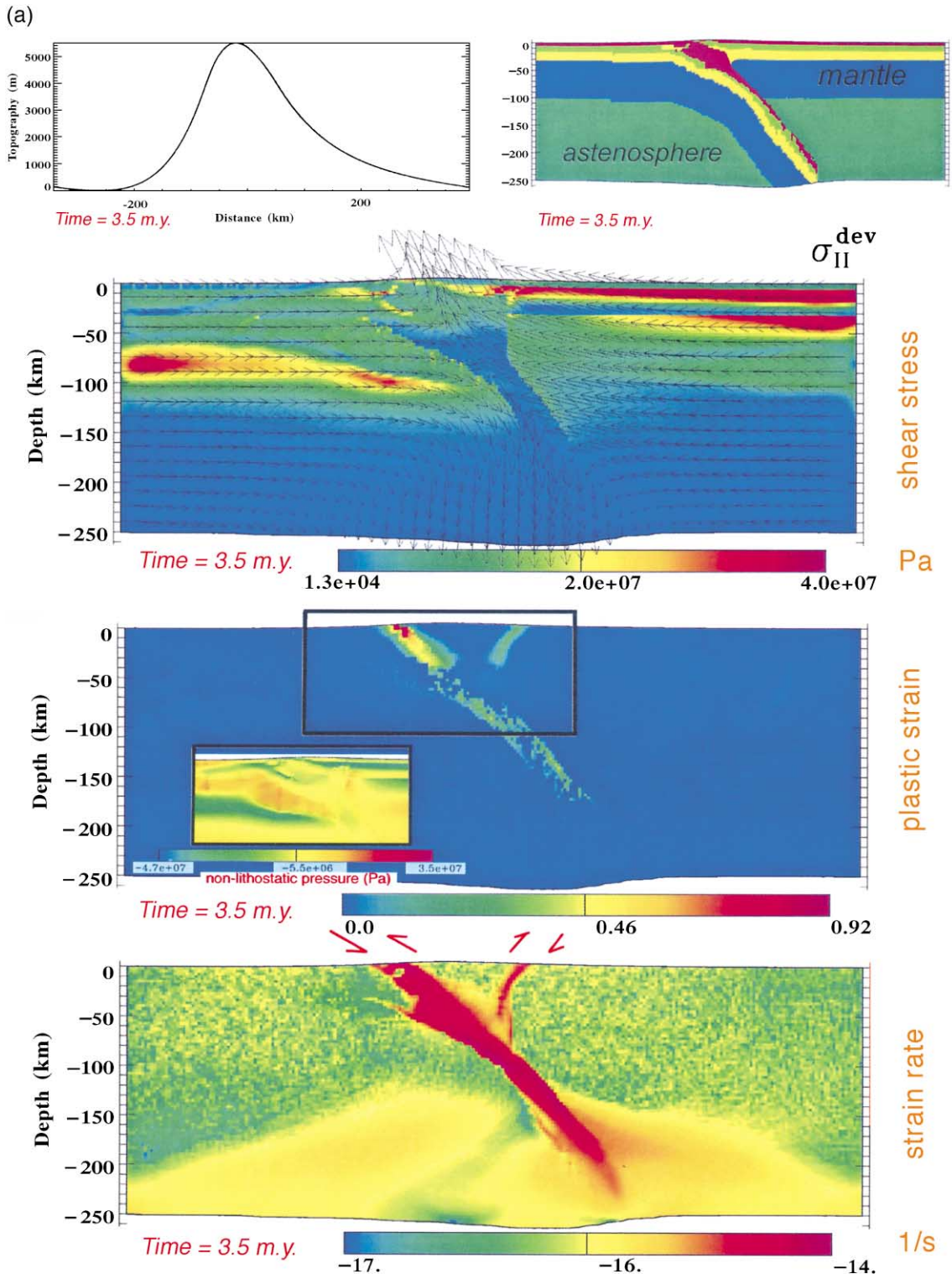
(a)
Topography (m)
5000
4000
3000
2000
1000
0
-200
200
Distance (km)
Time = 3.5 m.y.
mantle
astenosphere
Time = 3.5 m.y.
σ_{II}^{dev}
Depth (km)
0
−50
−100
−150
−200
−250
Time = 3.5 m.y.
1.3e+04
2.0e+07
4.0e+07
shear stress
Pa
−4.7e+07
−5.5e+06
3.5e+07
non-lithostatic pressure (Pa)
Time = 3.5 m.y.
0.0
0.46
0.92
plastic strain
Time = 3.5 m.y.
−17.
−16.
−14.
strain rate
1/s

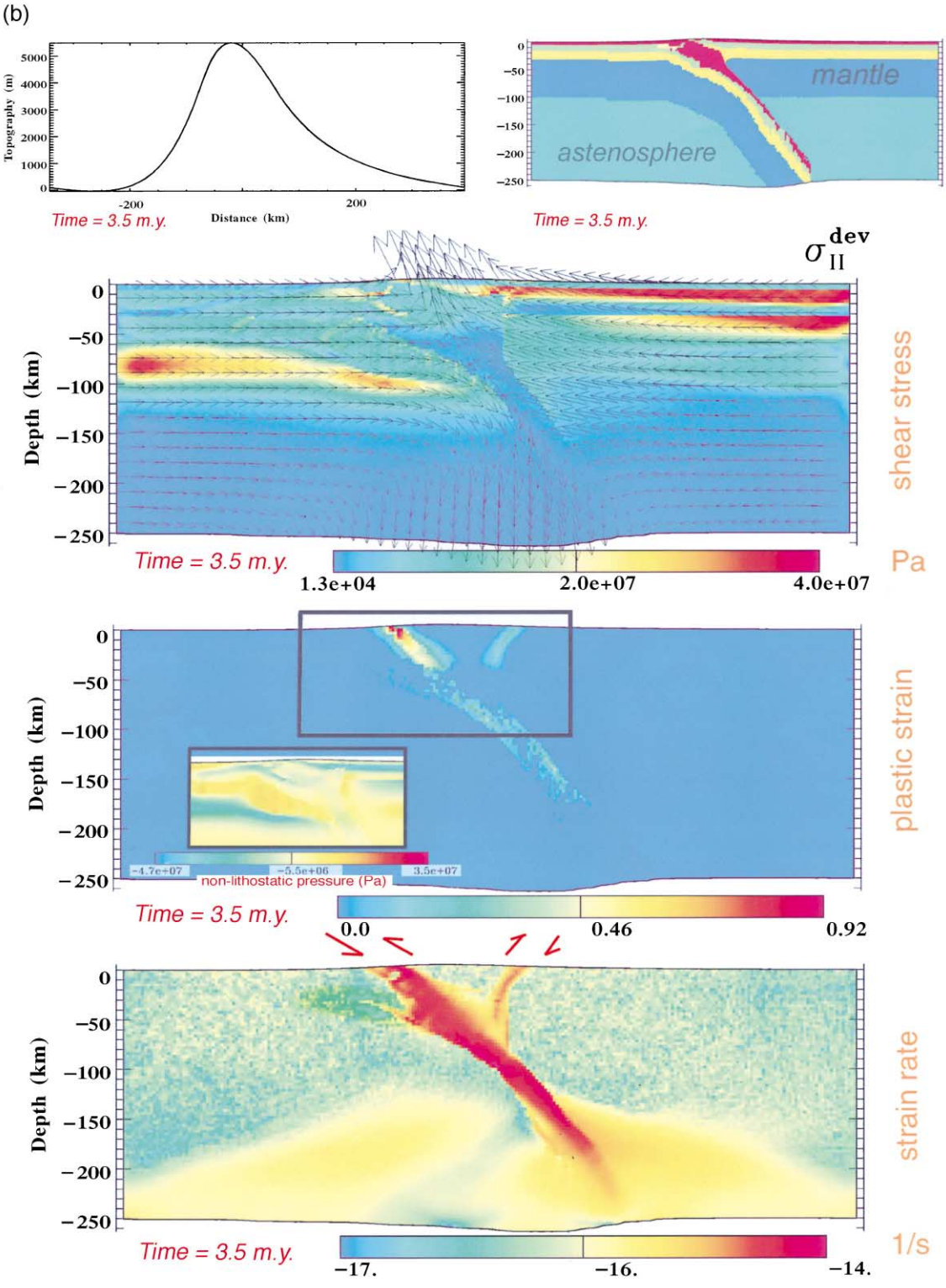
(b)
Topography (m)
Distance (km)
Time = 3.5 m.y.
mantle
astenosphere
Time = 3.5 m.y.
σ_{II}^{dev}
Depth (km)
shear stress
Time = 3.5 m.y.
1.3e+04
2.0e+07
4.0e+07
Pa
plastic strain
non-lithostatic pressure (Pa)
Time = 3.5 m.y.
0.0
0.46
0.92
strain rate
Time = 3.5 m.y.
−17.
−16.
−14.
1/s

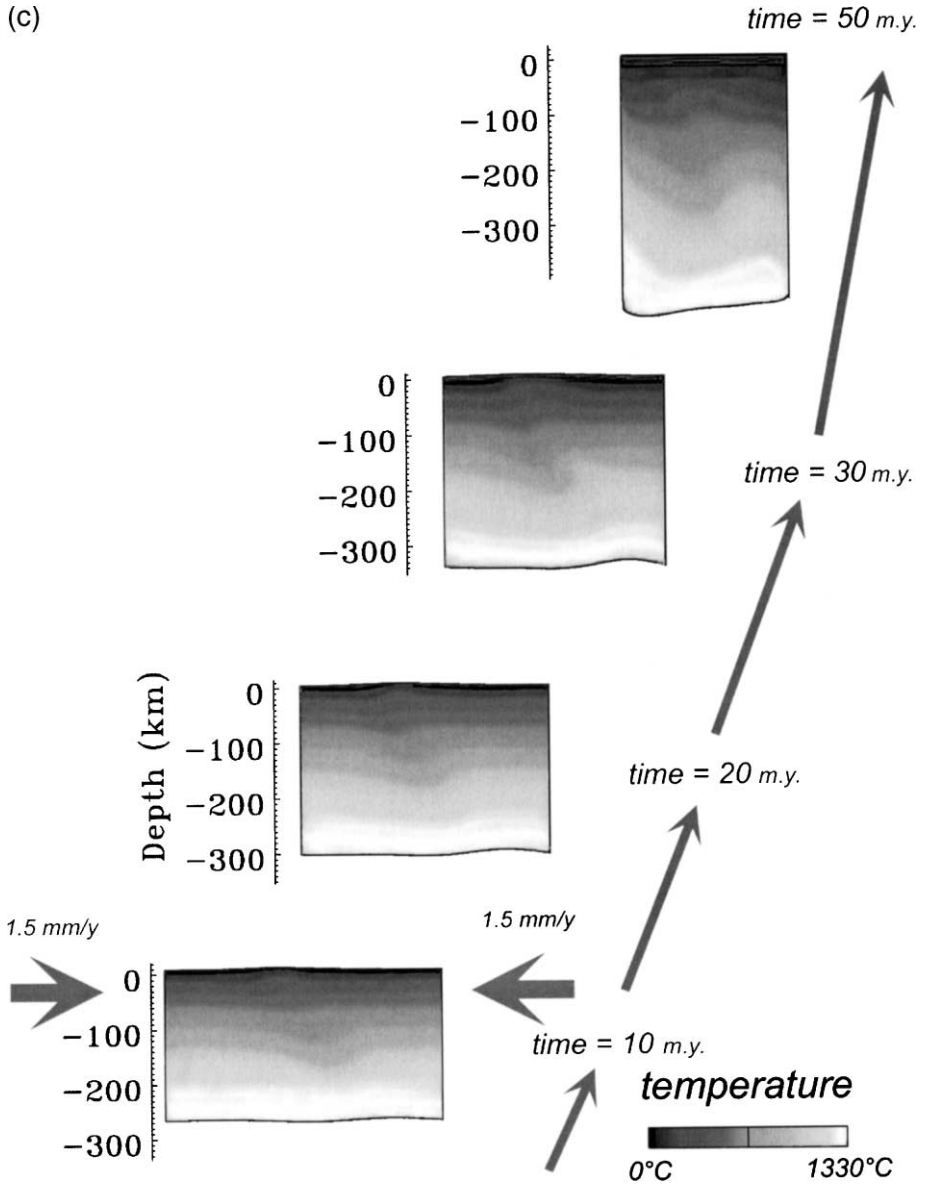

detachment. Yet in the experiment, no "geometrical" detachment of the subducting slab has occurred. Instead, the plastic hinge develops in a narrow necking zone extending like a chewing gum to very important depths without actual disrupting. Since the mechanical strength of this neck is extremely low, the downgoing part of the slab is mechanically disconnected from the upper part of the lithosphere, which is similar to the effect of the slab break-off.

3.1.5. Three-floor circulation

The upper and lower crustal accumulation zones, which we will later also call "chambers", demonstrate quite different behaviors. The material in the upper crustal chamber undergoes a two-floor circulation. The first floor involves corner-flow-like circulation of the sedimentary matter and of some upper crustal material, and is limited to 30-km depth. The second floor is limited to 70-km depth and involves mostly

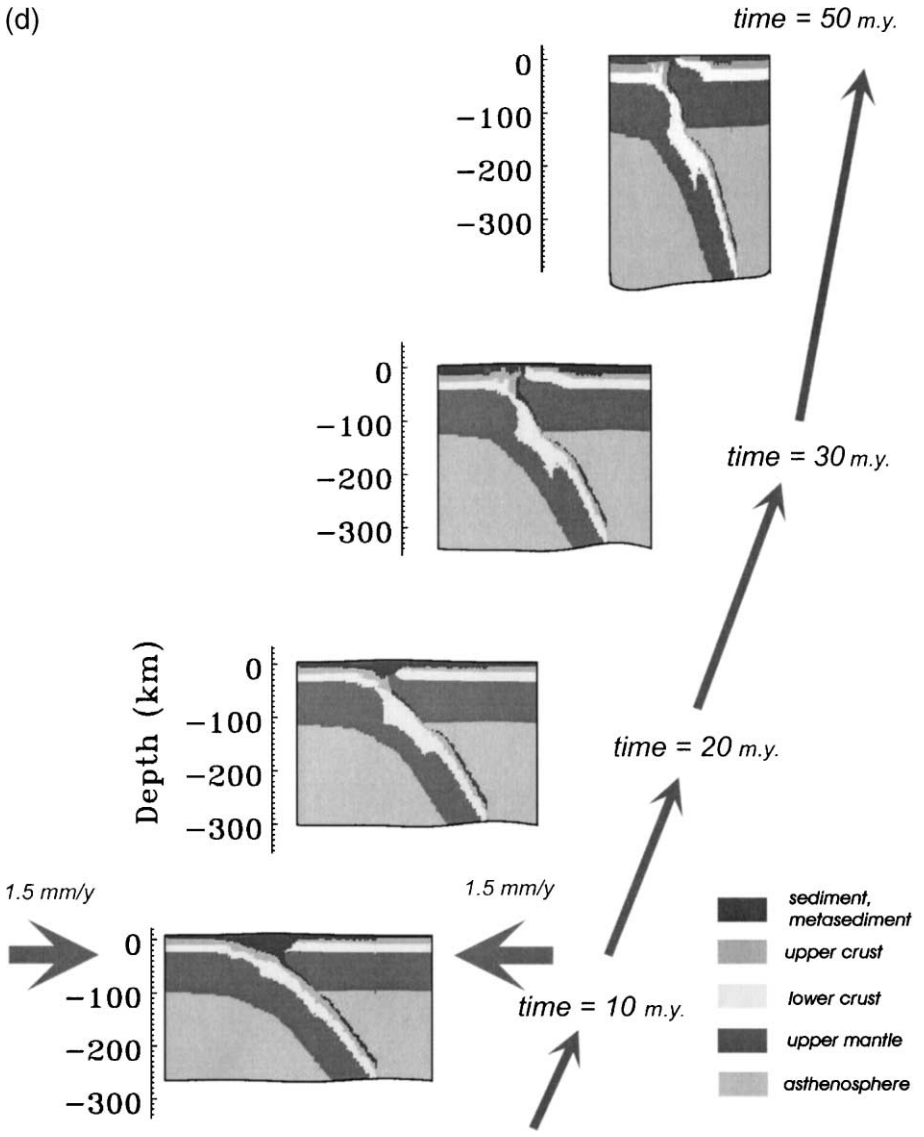

lower and partly upper crust. The 70-km depth corresponds to the beginning of the crustal "neck" separating the upper crustal wedge and the lower crustal chamber. The material transported with the mantle lithosphere from the upper crustal wedge to the lower chamber (Figs. 2 and 3) down to depths of 120 km, is then rapidly returned back from the lower chamber (ultra-high pressure exhumation). The rates of the crustal flow in the lower crustal chamber can be quite different from the subduction rate. When the chamber thickens, the flow of a part of the material in it is slowed down resulting in more effective conductive heating from the neighboring asthenosphere. As a result, the crustal viscosity drops, thus promoting a convective circulation in the chamber, which results in ascent of deep crustal material back to the valve neck area. From here, the material is squeezed further upward to the upper crustal chamber. From this chamber, the material is brought to the surface by the corner-flow-like circulation mechanism.

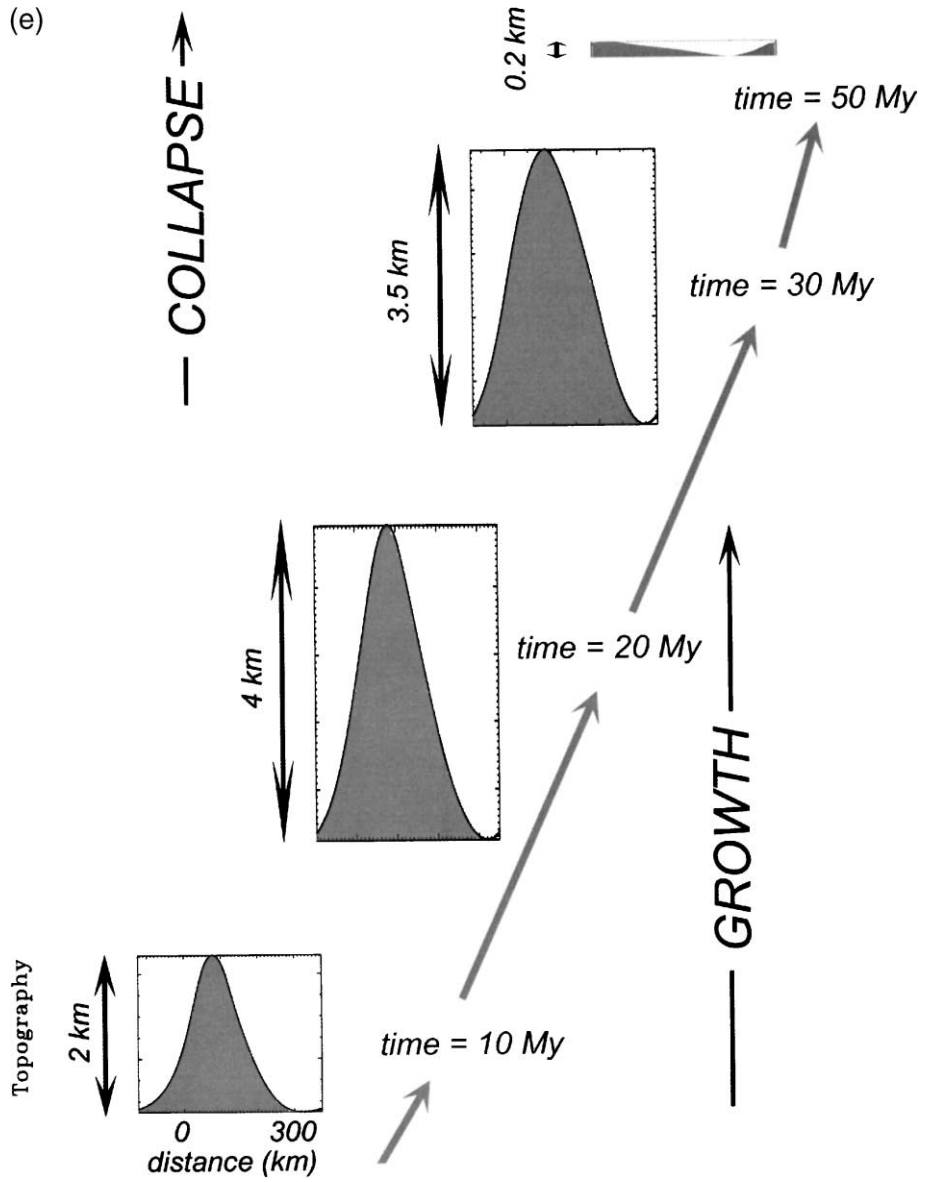

Fig. 2. Slow shortening rate experiments (3 mm/year) assuming high eclogitization (low buoyancy, see text). (a) Early stages of collision (3.5 m.y.): from top to bottom—topography, lithological structure, shear stress (second invariant) and velocity vectors, plastic strain and non-lithostatic pressure (in a rectangular insert), strain rate pattern. Note the formation of the non-predefined backthrust soon after initiation of subduction. Color code for the lithological structure: asthenosphere (dark green); mantle (blue); lower crust (dark yellow); upper crust (salad green); sediment, metasediment and reworked surface material (violet/bordeaux). (b,c,d) Consecutive stages of deformation (0–50 m.y.): lithology (b), temperature (c), topography (d). Note the formation of the plastic hinge in the downgoing plate and of the two "crustal chambers".

The "fast" experiment in Fig. 4 corresponds to shortening rate of 6 mm/year, which is the maximum rate expected for Alpine collision. The basic difference from the previous experiment is in the "stronger" response of the system (high strain rate results in higher stress in the ductile portions of the lithosphere)

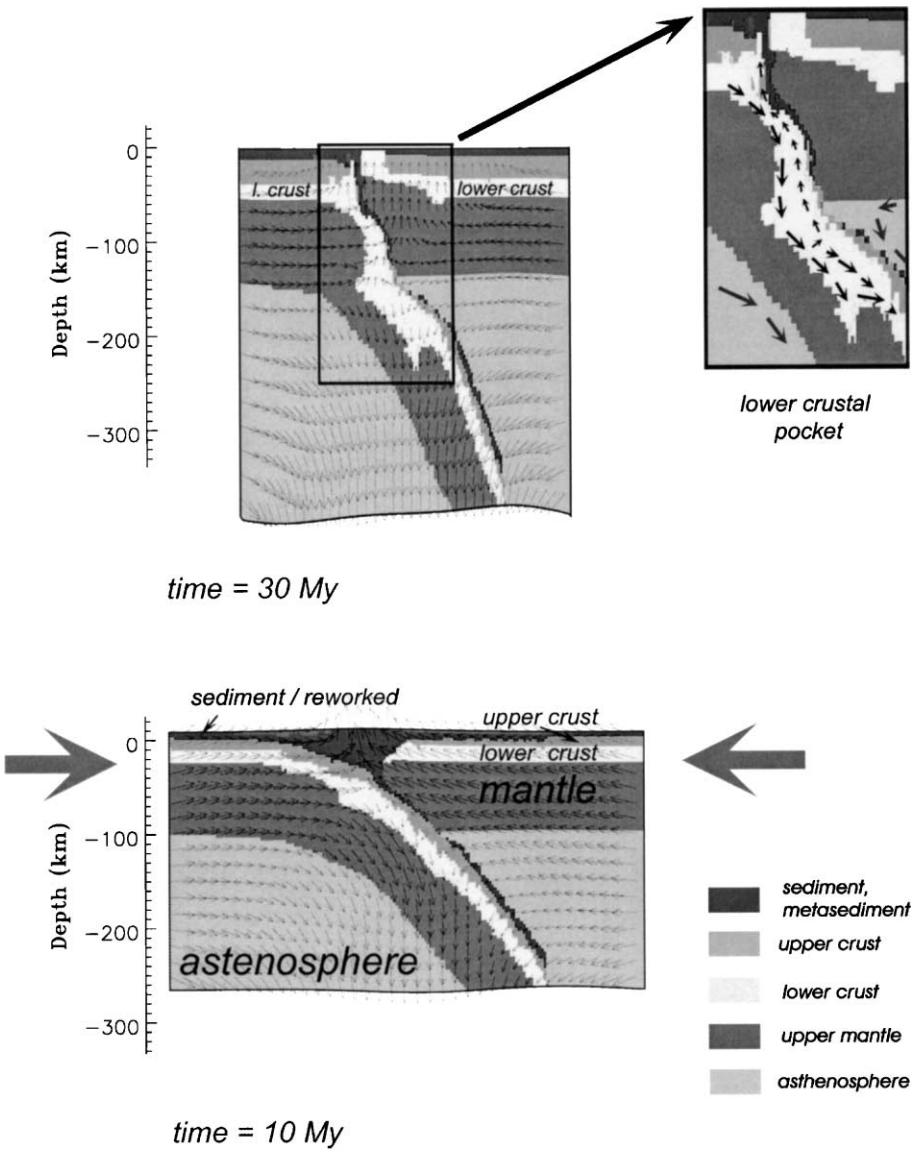

Fig. 3. A zoom to the lithological structure showing multi-level material circulation in the subducting crust and the accretionary prism on developed stages of collision. Arrows correspond to velocity vectors. Other notations are the same as in Fig. 2a.

and in reduced effect of the astenospheric heating on the development of instabilities in the lower crustal chamber.

Experiments from Figs. 2 and 3 (weak lower crustal rheology) show the development of a fold at the interface between the lower crust and upper crust. This fold verges toward the external zones and a piece of lower crust creeps upward between a thrust and an extensional shear zone. This fold is similar, to a first approach, to a Penninic nappe. Such a structure would probably not develop if the real density changes were taken into account and if recrystallization of granulite to eclogite were complete, that is, with final eclogite density higher than mantle one. However, this process

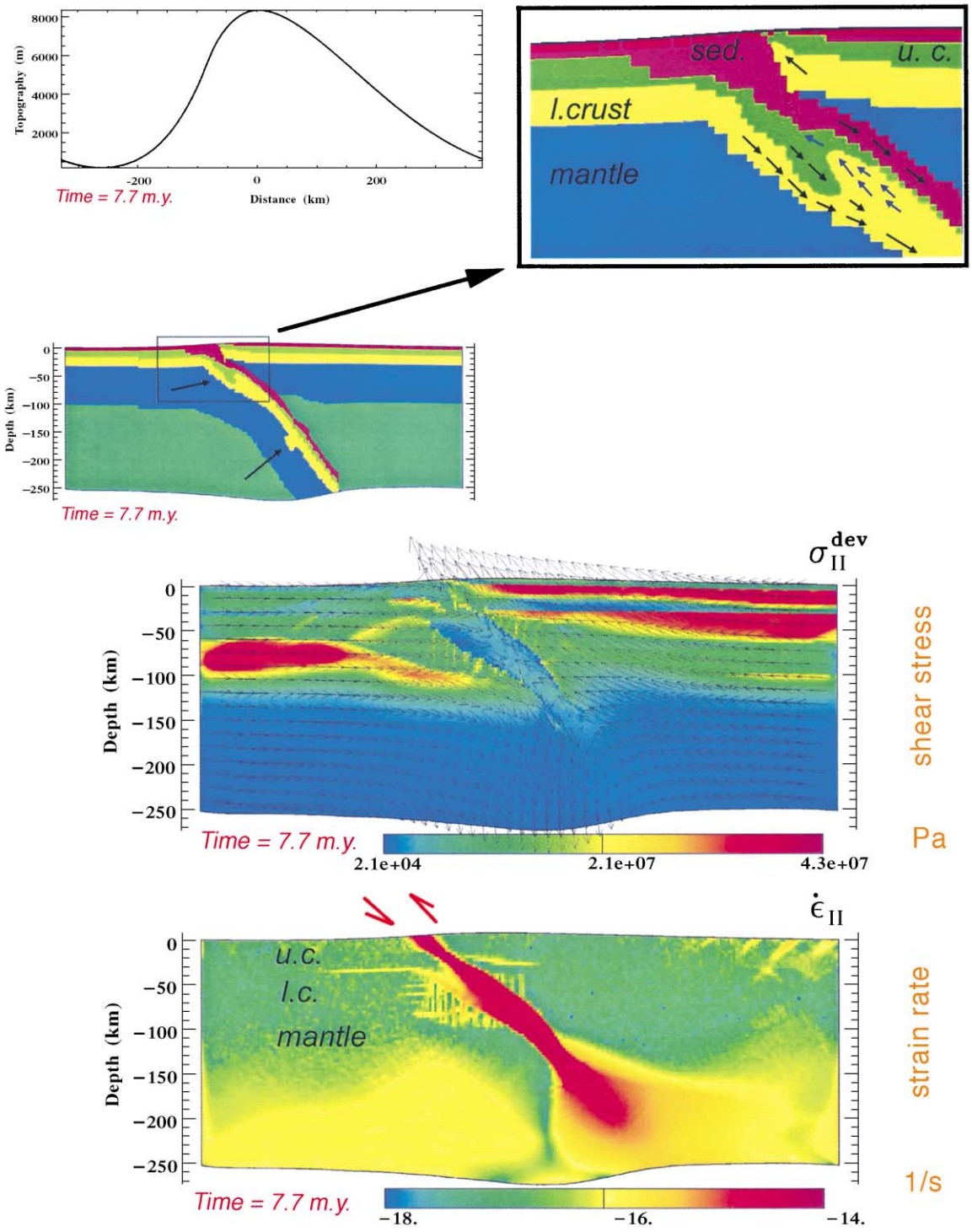

Fig. 4. Fast shortening rate experiments (6 mm/year). All notations are the same as in Fig. 2a.

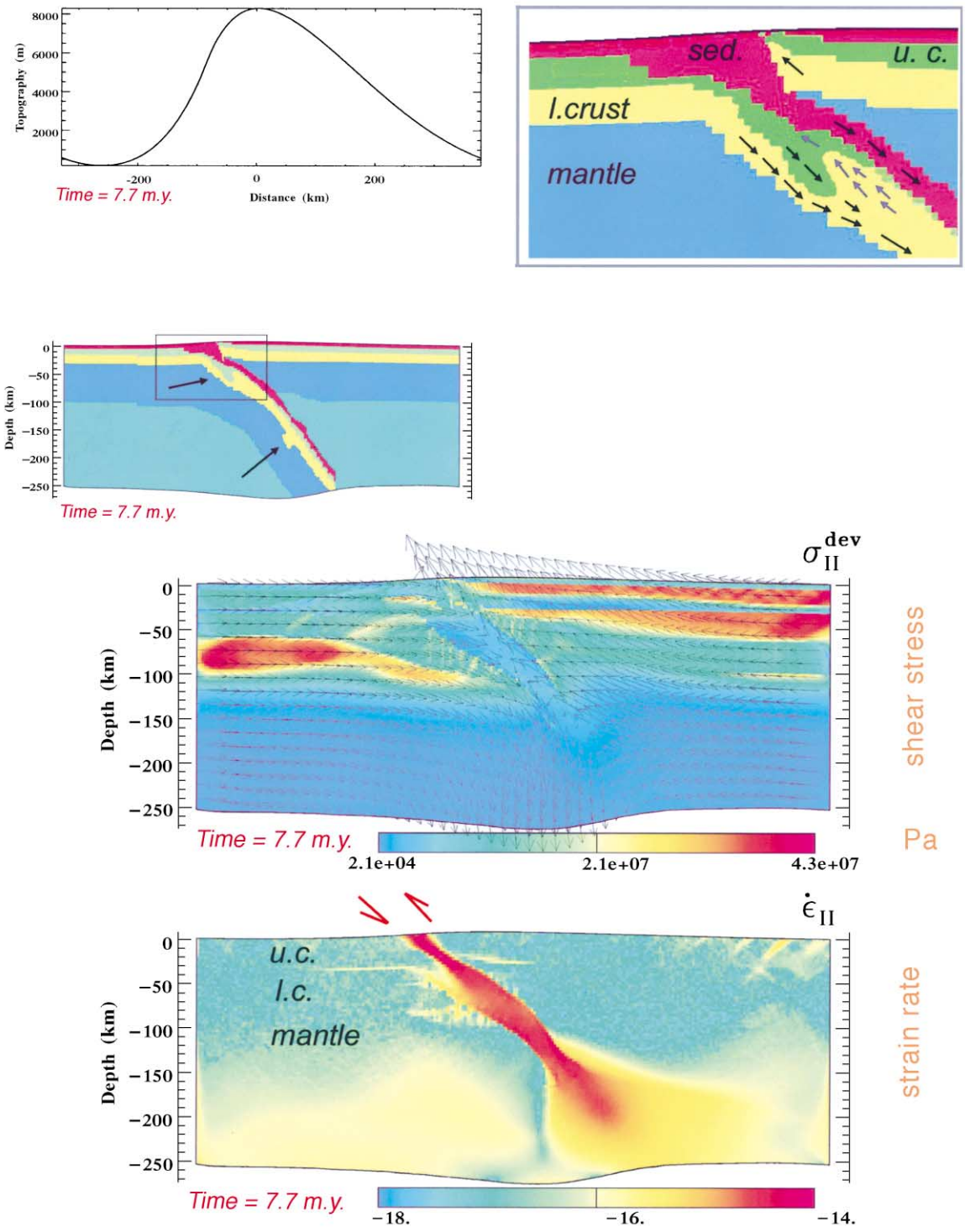

Fig. 4 (*continued*).

may explain some of the HP basement nappes of the Caledonides or the Penninic nappes of the Swiss Alps.

3.2. High-buoyancy mechanisms

In case of low eclogitization, the exhumation of HP rocks occurs in a much simpler way than in the previous scenario, for the buoyancy-driven forces, RT instabilities and convective heat transfer are extremely important and thus "handy" for upward transport of the crustal material. Fig. 5 shows the results of such experiments (all other parameters are the same as for the experiments in Figs. 2 and 3). Contrary to what happens in the previous "full eclogitization" case, the crust is not dragged down to important depth, because the heat and positive buoyancy result in its decoupling and extremely rapid return to the surface. This return is followed by decoupling and roll-back of both subducting and overriding plate. Contrary to most roll-back mechanisms, the experiment predicts that intensive convective flow of the upwelling hot asthenosphere below the overriding plate occurs in the direction opposite to that of convergence (Fig. 5). Although a similar effect was suggested by Gvirtzman and Nur (1999), these authors proposed a different mechanism for the asthenospheric upwelling (slab-roll back and rebound of the overriding plate). In case of a "light" slightly eclogitized or acidic crust, the upper crust most likely remains at the surface, whereas the lower crust is unlikely to be tracked deeper than 120- to 150-km depths. Contrarily, crustal detachment and return of a part of the crustal material to the surface occurs at earlier stages of subduction. A plastic hinge forms as in the previous case, but the slab at the beginning tends to bend upward, that is toward the overriding plate, and forms a near horizontal step-like turn underthrusting the overriding plate. The slab then bends down at some important horizontal distance below the overriding plate. The provoked asthenospheric upwelling enhances reheating and upward dragging of the subducting crust to the surface. This slab/asthenosphere motion together with the roll-back of the overriding plate result in "suction" of the returning extremely ductilized lower crustal material toward the surface, and not in its accumulation below the overriding plate as could be derived from some previous models (e.g., Chemenda et al., 1995, 1996).

3.2.1. Plastic hinging

In the high-buoyancy case, there are to plastic hinges forming in the lower plate. The first plastic hinge forms approximately in the same area as in the low buoyancy case. Yet, this time is caused by buoyancy-driven upward flexure of the lower plate. This upward flexure results from positive flexural moment created by low density portion of the downgoing crust, which is not yet decoupled from the mantle lithosphere. At later stages, when crustal decoupling occurs, the mantle slab starts to bend down under its own weight, forming a second plastic hinge at some horizontal distance from the first plastic hinge. This distance is conditioned by the load of the decoupled part of the slab, by the density contrast between the crust and the mantle, and by resistance of the crust to decoupling. The lower plate takes a quasi-steady geometry with a step-like horizontal turn underneath the overriding slab and can easily horizontally underthrust it by several hundred kilometers. The slab bending around the two plastic hinges is controlled by several factors: ratio of the volume of the non-decoupled crust to that of the subducting slab, subduction rate and the overall convective motion in the asthenosphere. It is yet clear that the first plastic hinging should occur at depths of about 100–120 km and result in formation of the lower crustal chamber and in "extended" slab break off zone.

3.2.2. Corner flow at the upper level and convection-like crustal circulation at the lower level

In the high-buoyancy case, the shallow corner flow exhumation mechanism (depths up to 30–40 km) is preserved, as in the previous low-buoyancy case. The second level (70 km) circulation does not occur since it is overprinted by faster flow due to strong buoyancy contrast and by thermal convection flow, which takes place in the whole crustal channel below 40-km depth.

3.2.3. Normal shear zone and previous models

The high-buoyancy experiment shows a very fast (several times the shortening rate) exhumation of ductilized material from important depths. Indeed, even very rough analytical estimations demonstrate enormous efficiency of the thermal instability mechanism in case of non-linear rheology, especially if one assumes that part of a quart-controlled crust ascends through the crustal embeddings. As a first approxi-

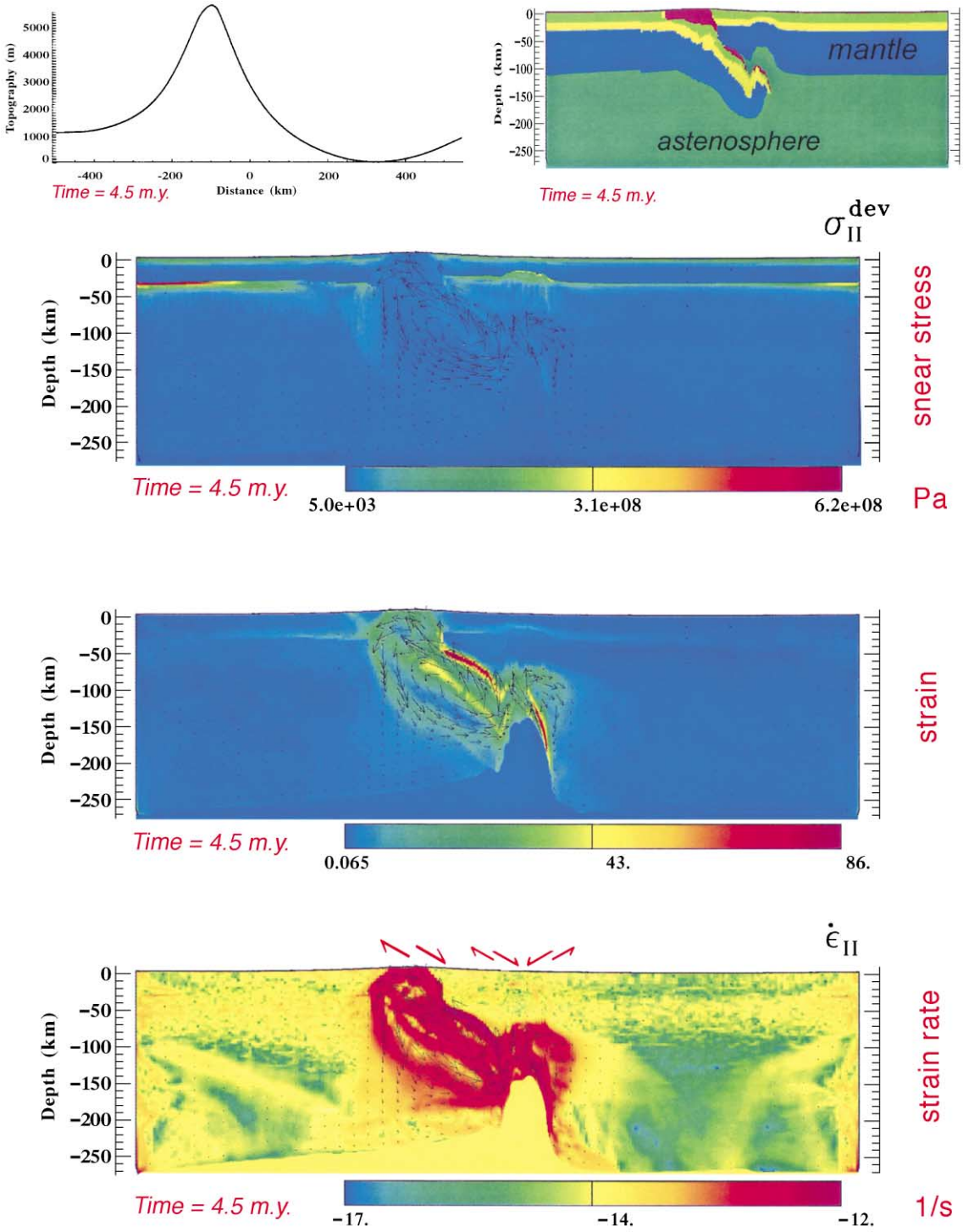

Fig. 5. Low eclogitization (high buoyancy) experiment (see text). The notations are as in Fig. 2a, except that the strain part of this figure does not show plastic but total accumulated strain (to better the emphasize the ductile shear zone at depth).

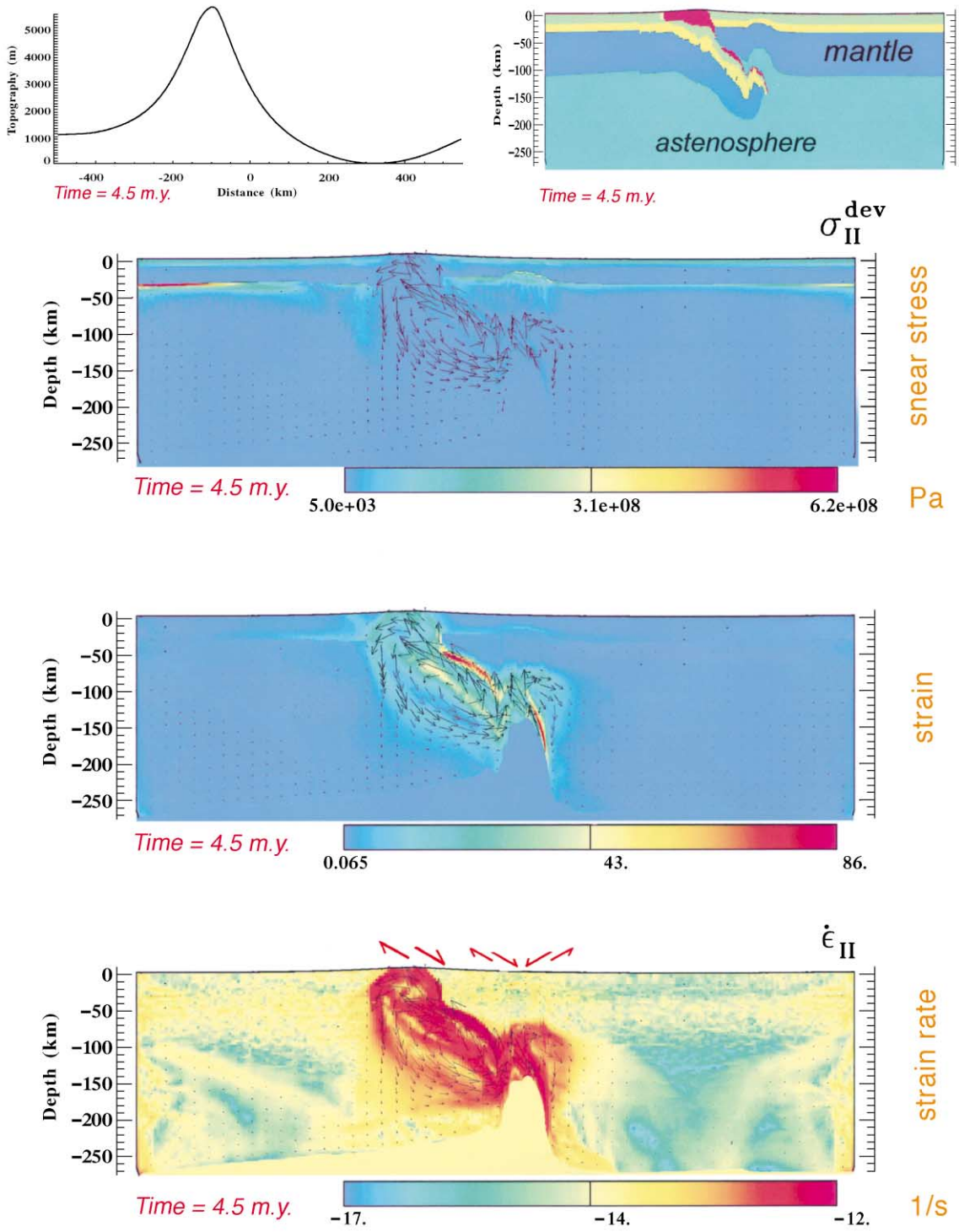

Fig. 5 (*continued*).

mation, we can use the equation for the ascent velocity (v_y) of a translating sphere (Stokes problem) extended by Weinberg and Podladchikov (1994) for the case of non-linear rheology, which effective viscosity μ_{eff} is derived assuming characteristic buoyancy-driven stress $\sigma=\Delta\rho gr$:

$$\partial\varepsilon/\partial t = \sigma^n A\exp(H/RT)$$

$$\mu_{\text{eff}} = (6^{n-1}\exp(H/RT))/(3^{1/2(n-1)}A(\Delta\rho gr)^{n-1})$$

$$v_y = \Delta\rho gr^2/3\mu_{\text{eff}} = 3^{1/2(n-1)}rA(\Delta\rho gr)^n/(3\times 6^{n-1}\exp(H/RT))$$

where r is the approximate radius (half-thickness) of the ascending crustal body; $\partial\varepsilon/\partial t$ is the strain rate; n, A, H, T is the power law exponent, material constant, activation enthalpy and temperature of the embeddings, respectively; R is the gas constant (8.314 J mol^{-1} °C^{-1}); g is the acceleration due to gravity (9.8 m s^{-2}); and $\Delta\rho$ is the density contrast. For example, $\Delta\rho$ can be $\Delta\rho=\alpha\rho_0\Delta T$ where α is the coefficient of thermal expansion (typically 3×10^{-5} °C^{-1}), ρ_0 is the material density at 0 °C and ΔT is the temperature contrast with the embeddings. Let us consider following typical conditions: background temperatures of about 600 °C, $\Delta\rho$ ranging from 20 to 200 kg m^{-3} and temperature contrasts between the ascending material and embeddings ranging from 100 to 300 °C. Whatever the embedding is, quartz-rich crust (n=3, H=190 k J mol^{-1}, $A=5\times10^{-12}$ Pa^{-n} s^{-1}, ρ_0=2600÷2900 kg m^3) or mantle olivine (n=3, H=520 k J mol^{-1}, $A=7\times10^{-14}$ Pa^{-n} s^{-1}, ρ=3300 kg m^{-3}) (Burov et al., 1999)), one can find that these conditions would be largely sufficient to drive up a 20-km thick body at 10–20 cm/year. For larger temperature or density contrasts, the estimated values of v_y become incredibly high, suggesting the possibility of very fast material ascent at great depth, which would slow down near the surface due to decreasing temperature. Naturally, these estimates are highly sensitive to the material parameters, for example in case of a crustal quartzite-rich body ascending through olivine background ($\Delta\rho$=430 kg m^{-3}), the ascendance rate may vary from 10^{-3} mm/year for embedding temperature of 700 °C to 10^3 mm/year for embedding temperature of 900 °C. In case of more temperature sensitive quartzite embeddings (hot crust material ascends through cold crustal embeddings), the scatter in possible vertical velocities becomes very important, including a possibility of fast turbulent flow inside and outside of the crustal body.

The velocity contrast between the exhuming material and the mantle and crustal material of the upper plate induces formation of a large-scale shear zone, which works as a normal fault with a relative upward motion of the footwall. This is quite similar at a first glance to what Chemenda et al. (1995, 1996, 1997) have obtained from analogue laboratory experiments. There are however some principal differences between the two models. In the Chemenda model, continental crust is exhumed as a large rigid block, which decouples from the mantle and glides up between the downgoing slab and the upper plate. This ascent is driven by density contrast between the crust and mantle. In this model, the exhumed body presents a rigid crustal block included between a thrust zone forming along the Moho boundary of the lower plate and a normal fault zone forming between the lower and upper plate. In our experiments, the exhumed material is not rigid, but highly ductilized due to high temperature. Contrary to that, the Chemenda model is incompatible with the possibility of long exposure of the subducted crust to high temperatures. The second important difference relates to the geometry of the downgoing slab. In the numerical high-buoyancy experiment, the downgoing slab has a tendency to rotate upward below the upper plate, due to a positive flexural moment created by cumulative effect of remaining low density crustal layer and of asthenospheric upflow below the overriding plate. The third principal difference is that in the present model there is no important accumulation of crustal material below the upper plate as would be observed in the Chemenda model in case of weak crustal rheology or hot surroundings. The fourth, less important difference is related to the presence of active extension within the upper plate provoked by the upwelling asthenosphere.

4. Discussion and conclusions

The summary of results is shown in Fig. 6. In the case of low buoyancy (high eclogitization, Fig. 6a), the subducted crust is likely to be subdivided on two

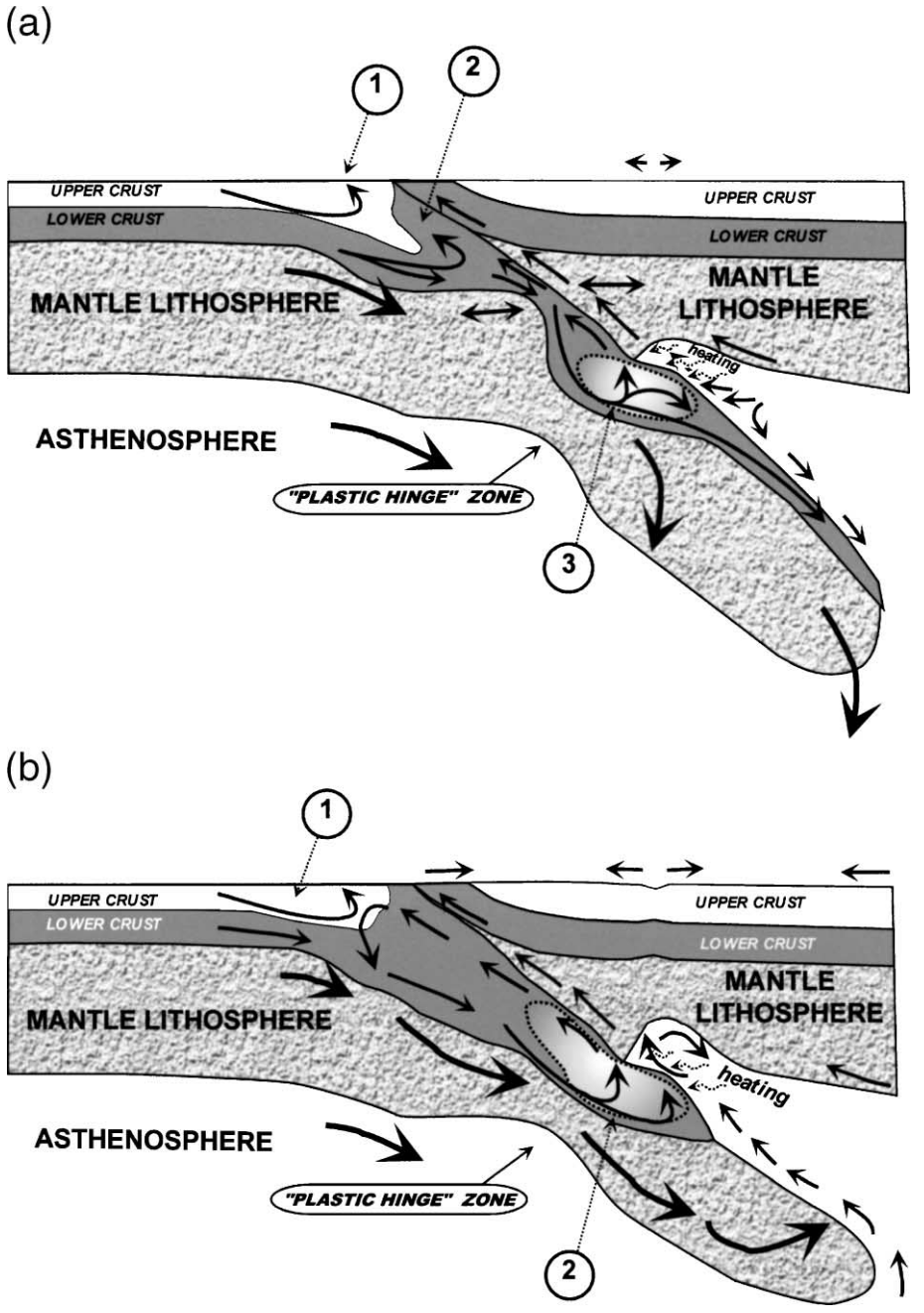

Fig. 6. Schematic illustration summarizing general results of this study. (a) Full eclogitization (low buoyancy) case. Three mechanisms and levels of exhumation are predicted: 1. LP–LT corner flow exhumation (up to 40-km depth); 2. HP–HT exhumation from the upper crustal chamber; 3. UHP–UHT/HP–HT exhumation from the lower crustal chamber by a slow convective instability and overriding plate drag. (b) Low eclogitization (high buoyancy) case. Two mechanisms and levels of exhumation are predicted: 1. LP–LT corner flow exhumation (up to 40-km depth); 2. UHP–UHT/HP–HT exhumation of the subducted lower crust by a fast convective instability and drag by overriding plate. Note also the active extension in the overriding plate produced by the upwelling asthenosphere.

thickened zones: the upper crustal wedge, or chamber, above the 70-km depth, and the lower crustal chamber (up to 120- to 150-km depth). As long as the subduction continues, the slab approaches a prebreak-off condition, which is initiated by flexural plastic hinging (yielding) (Burov and Diament, 1995) located in the depth interval between 70–80 and 130 km. Hinging results in localized mantle lithospheric thinning and stretching in the hinge area, like a honey or chewing gum. The thinner this area becomes, the faster it heats up from the surrounding asthenosphere, and consequently the faster it weakens. As a result, the lower crustal chamber can be also stretched and ruptured. One completely metamorphosed part of it goes down with the descending slab, whereas another part stays above just below the ''nozzle'' area. A ''real'' slab break-off may never occur, since the slab thins and weakens in the hinge zone until it is unable to transfer any considerable stress to the uppermost lithosphere. The uppermost lithosphere is thus progressively unloaded, which results in post-collision rebound followed by orogenic collapse on the side of the overriding plate.

One of the primary conclusions that we may draw out from this study states that in case of high degree of metamorphism, rock exhumation from different depth levels can be effectuated by three depth-specific mechanisms. These mechanisms are different but highly interdependent.

1. Depths interval of 0–30 km and temperature interval of 0–500 °C: classical corner flow mechanism, LP–LT conditions. The exhumation rates for this mechanism are smaller than those of tectonic shortening.

2. Depths interval of 30–70 km and temperature interval of 300–700 °C: positive buoyancy forcing and material dragging by the overriding plate. HP–HT conditions. The exhumation rates for this mechanism are close to those of tectonic shortening.

3. Depth interval of 40–120 km and temperature interval of 500–900 °C: small-scale convection in the lower crustal chamber, dragging and injection of the material from the lower crustal chamber into the upper crustal wedge. UHP–UHT/HP–HT conditions. The exhumation rates for this mechanism generally exceed those of tectonic shortening and are not directly controlled by it.

Although the upper and lower crustal accumulation zones and the narrow channel between them resemble a vortex-shaped nozzle with the upper crustal wedge geometrically resembling combustion chamber of a jet engine, no physical analogies can be drawn. In reality, this system cannot function as a jet nozzle as suggested in (Mancktelow, 1995), because the ''nozzle'' walls are too deformable and cannot maintain overpressures in excess of 20–40 MPa. In our model, the function of the narrow bypass between the thickened upper and crustal chambers is to control the amount of material that can be exchanged in the upward and downward direction between the crustal accumulation zones.

In the low eclogitization case (Fig. 6b), crust is likely to decouple from the subducting mantle on the early stages of subduction. It can be dragged only to 80–120 km depth and then returns to the surface at rates that may exceed several times the tectonic shortening rates in case of large density contrasts. The positive buoyancy forces applied to the subducting crust result in upward rotation of the slab around the plastic hinge zone. This rotation, first, temporarily accelerates subduction of the mantle slab, then retards it, and provokes asthenospheric upwelling towards the corner between the subducting and overriding plates. The initiated astenospheric convective cell results decollement of the overriding plate and its extension at some distance from the collision zone. The comparison between the two end-member models also suggests that the exhumation mechanism proposed by Chemenda et al. (1995) may work in the case of high-buoyancy crust but is unlikely to work in case of a low buoyancy crust. It is thus important for coming studies to consider the influence of phase changes and possible significant increase of density at crustal scale.

In the high-buoyancy model (Fig. 6b), active upwelling of the asthenospheric material induces high heat flow and extension in the upper plate. The general situation depicted by the high-buoyancy model is quite similar to the Neogene kinematics of the Himalayan–Tibet region, which is characterized by frontal thrusting and upper plate extension behind a major extensional shear zone (North Tibetan Detachment Zone (Burchfiel et al., 1992; Burg et al., 1984)). If one assumes that the subducted crust in the Himalayan–Tibet convergence zone is not pervasively eclogitized, this mechanism could explain the high heat flow, volcanism (Turner et al., 1996) and extension (Armijo et al., 1986; Molnar and Lyon-

Caen, 1989) recorded at present in the Tibetan plateau, besides classical models of convective removal (England, 1993). Because of the low rate of eclogitization required, this model opposes the alternative models where dense eclogitized lower crust is stoked in the upper mantle below the Tibetan plateau (Le Pichon et al., 1997). It is too early to be conclusive on this ground, but we suggest that this numerical experiment provides an additional mechanism to be considered in the future.

Acknowledgements

We deeply thank Dr. S. Wdowinski for critical review and highly constructive detailed comments. We also thank Prof. S. Cloetingh for very useful review and Prof. P. Ziegler for critical comments on the model. We also had encouraging discussions with Drs. Ph. Philippot, Y. Podladchikov, A. Perchouk and Profs. A. Chemenda and C. Fascena. This is INSU contribution No. 284.

References

Agard, P., Jolivet, L., Goffé, B., 1999. The Schistes Lustrés complex: a key for understanding the exhumation of HP and UHP rocks in the Western Alps. Tectonophysics submitted.

Andersen, T.B., 1998. Extensional tectonics in the Caledonides of southern Norway, an overview. Tectonophysics 285, 333–352.

Andersen, T.B., Jamtveit, B., 1990. Uplift of deep crust during orogenic extensional collapse: a model based on field studies in the Sogn–Sunnfjord region of Western Norway. Tectonics 9, 1097–1111.

Andersen, T.B., Osmundsen, P.T., Jolivet, L., 1994. Deep crustal fabric and a model for the extensional collapse of the southwest Norwegian Caledonides. J. Struct. Geol. 16, 1191–1203.

Armijo, R., Tapponnier, P., Mercier, J.L., Tonglin, H., 1986. Quaternary extension in southern Tibet: field observations and tectonic implications. J. Geophys. Res. 91, 13803–13872.

Austrheim, H., Boundy, T., 1994. Pseudotachylites generated during seismic faulting and eclogitization of the deep crust. Science 265, 82–83.

Austrheim, H., Erambert, M., Engvik, A.K., 1997. Processing of crust in the root of the Caledonian continental collision zone: the role of eclogitization. Tectonophysics 273, 129–154.

Avouac, J.P., Burov, E.B., 1996. Erosion as a driving mechanism of intracontinental mountain growth. J. Geophys. Res. 110, 17747–17769.

Ballèvre, M., Merle, O., 1993. The Combin Fault: compressional reactivation of a Late Cretaceous–Early Tertiary detachment fault in the Western Alps. Schweiz. Mineral. Petrogr. Mitt. 73, 205–227.

Ballèvre, M., Lagabrielle, Y., Merle, O., 1990. Tertiary ductile normal faulting as a consequence of lithospheric stacking in the Western Alps. Mem. Soc. Geol. Fr. 156, 227–236.

Beukel, J., 1992. Some thermomechanical aspects of the subduction of continental lithosphere. Tectonics 11, 316–329.

Boundy, T.M., Hall, C.M., Li, G., Essene, E.J., Halliday, A.N., 1997. Fine-scale isotopic heterogeneities and fluids in the deep crust; a 40Ar/39Ar laser ablation and TEM study of muscovites from a granulite–eclogite transition zone. Earth Planet. Sci. Lett. 148, 223–242.

Bousquet, R., Goffé, B., Henry, P., Le Pichon, X., Chopin, C., 1997. Kinematic, thermal and petrological model of the Central Alps: Lepontine metamorphism in the Upper Crust and eclogitisation of the lower crust. Tectonophysics 273, 105–128.

Bousquet, R., Oberhänsli, R., Goffé, B., Jolivet, L., Vidal, O., 1998. Distribution of HP–LT metamorphism and extensional deformation in the "Bündnerschiefer" of the Engadine window (eastern Central Alps): implications for regional evolution. J. Metamorph. Geol. 16, 653–670.

Brown, D., Juhlin, C., Alvarez-Marron, J., Perez-Estaun, A., Oslinshi, A., 1998. Crustal scale structure and evolution of an arc–continent collision zone in the southern Urals, Russia. Tectonics 17, 158–171.

Burchfiel, B.C., Zhiliang, C., Hodges, K.V., Yuping, L., Royden, L.H., Changrong, D., Jiene, X., 1992. The south Tibetan detachment system, Himalayan orogen: extension contemporaneous with and parallel to shortening in a collisional mountain belt. Geol. Soc. Am., Spec. Pap. 269, 1–41.

Burg, J.P., Guiraud, M., Chen, G.M., Li, G.C., 1984. Himalayan metamorphism and deformations in the North Himalayan Belt (southern Tibet, China). Earth Planet. Sci. Lett. 69, 391–400.

Burg, J.P., Podladchikov, Y., 1999. Lithospheric scale folding and rock exhumation: numerical modelling and application to the Himalayan syntaxes. In: Khan, M.A., Treloar, P.J., Searle, M.P., Jan, M.Q. (Eds.), Tectonics of the Nanga Parbat Syntaxis and the Western Himalaya. Geol. Soc. London Spec. Publ., vol. 170, pp. 219–236.

Burov, E.B., Cloetingh, S., 1997. Erosion and rift dynamics: new thermomechanical aspects of post-rift evolution of extensional basins. Earth Planet Sci. Lett. 150, 7–26.

Burov, E.B., Diament, M., 1995. Effective elastic thickness of the continental lithosphere—what does it really mean? J. Geophys. Res. 100, 3905–3927.

Burov, E.B., Diament, M., 1996. Isostasy, effective elastic thickness (EET) and inelastic rheology of continents and oceans. Geology 24, 419–423.

Burov, E., Guillou-Frottier, L., 1999. Thermomechanical behavior of large ash flow calderas. J. Geophys. Res. 104, 23081–23109.

Burov, E.B., Molnar, P., 1998. Gravity anomalies over the Ferghana Valley and intracontinental deformation. J. Geophys. Res. 103, 18137–18152.

Burov, E.B., Poliakov, A., 2001. Erosion and rheology controls on syn- and post-rift evolution: verifying old and new ideas using a fully coupled numerical model. J. Geophys. Res. 106, 16461–16481.

Burov, E.B., Lobkovsky, L.I., Cloetingh, S., Nikishin, A.M., 1993. Continental lithosphere folding in Central Asia (part II). Tectonophysics 226 (1–4), 73–87.

Burov, E.B., Mareschal, J.-G., Jaupart, C., 1998. Large scale crustal inhomogeneities and lithospheric strength in cratons. Earth Planet Sci. Lett. 164, 205–219.

Burov, E.B., Podladchikov, Y., Grandjean, G., 1999. Validation of multidisciplinary data using thermo-mechanical modelling: application to the Western and Northern Alps. Terra Nova 11, 124–131.

Chemenda, A.I., Mattauer, M., Malavieille, J., Bokun, A.N., 1995. A mechanism for syn-collision rock exhumation and associated normal faulting: results from physical modelling. Earth Planet. Sci. Lett. 132, 225–232.

Chemenda, A.I., Mattauer, M., Bokun, A.N., 1996. Continental subduction and a mechanism for exhumation of high-pressure metamorphic rocks: new modeling and field data from Oman. Earth Planet Sci. Lett. 143, 173–182.

Chemenda, A.I., Yang, R.K., Hsieh, C.H., Groholsky, A.L., 1997. Evolutionary model for the Taiwan collision based on physical modeling. Tectonophysics 274, 253–274.

Chopin, C., 1984. Coesite and pure pyrope in high-grade blueschists of the western Alps: a first record and some consequences. Contrib. Mineral. Petrol. 86, 107–118.

Chopin, C., Henry, C., Michard, A., 1991. Geology and petrology of the coesite-bearing terrain, Dora Maira massif, Western Alps. Eur. J. Mineral. 3, 263–291.

Cloetingh, S., Burov, E.B., Poliakov, A., 1999. Lithosphere folding: primary response to compression? (from central Asia to Paris Basin). Tectonics 18, 1064–1083.

Cundall, P.A., 1989. Numerical experiments on localization in frictional materials. Ing.-Arch. 59, 148–159.

Dewey, J.F., Ryan, P.D., Andersen, T.B., 1993. Orogenic uplift and collapse, crustal thickness, fabrics and metamorphic phase changes: the role of eclogites. In: Prichard, H.M., Alabaster, T., Harris, N.B.W., Neary, C.R. (Eds.), Magmatic Processes and Plate Tectonics. Geol. Soc. Spec. Publ., vol. 76, pp. 325–343.

Dobretsov, N.L., 1991. Blueschists and eclogites: a possible plate tectonics mechanism for their emplacement from the upper mantle. Tectonophysics 186, 253–268.

England, P., 1993. Convective removal of thermal boundary layer of thickened continental lithosphere: a brief summary of causes and consequences with special reference to the Cenozoic tectonics of the Tibetan plateau and surrounding regions. Tectonophysics 223, 67–73.

Engvik, A., Andersen, T.B., 2000. The progressive evolution of Caledonian deformation fabrics under eclogite and amphibolite facies at Vardalsneset, Western Gneiss Region, Norway. J. Metamorph. Geol. 18, 241–257.

Engvik, A.K., Austrheim, H., Andersen, T.B., 2000. Structural, mineralogical and petrophysical effects on deep crustal rocks of fluid-limited polymetamorphism, Western Gneiss Region. J. Geol. Soc. London 157, 121–134.

Ernst, W.G., Liou, J.G., 1995. Contrasting plate-tectonics styles of the Qinling–Dabie–Sulu and Franciscan metamorphic belts. Geology 23, 353–356.

Franke, W., 1998. Exhumation of HP rocks in the Saxothuringian belt: sedimentary and tectonic record. Gieben, 44–46.

Gerbault, M., Poliakov, A., Daignieres, M., 1998. Prediction of faulting from the theories of elasticity and plasticity: what are the limits? J. Struct. Geol. 20, 301–320.

Gerbault, M., Burov, E.B., Poliakov, A., Daignieres, M., 1999. Do faults trigger folding in the lithosphere? Geophys. Res. Lett. 26, 271–274.

Goffé, B., Chopin, C., 1986. High-pressure metamorphism in the Western Alps: zoneography of metapelites, chronology and consequences. Schweiz. Mineral. Petrogr. Mitt. 66, 41–52.

Gvirtzman, Z., Nur, A., 1999. Plate detachment, asthenosphere upwelling, and topography across subduction zones. Geology 27, 563–566.

Henry, P., Le Pichon, X., Goffé, B., 1997. Kinematic, thermal and petrological model of the Himalayas: constraints related to metamorphism within the underthrust Indian crust. Tectonophysics 273, 31–56.

Jolivet, L., Patriat, M., 1999. Ductile extension and the formation of the Aegean Sea. In: Durand, B., Jolivet, L., Horvàth, F., Séranne, M. (Eds.), Geol. Soc. Spec. Publ., vol. 156. Geological Society, London, 427–456.

Jolivet, L., Daniel, J.M., Truffert, C., Goffé, B., 1994. Exhumation of deep crustal metamorphic rocks and crustal extension in back-arc regions. Lithos. 33, 3–30.

Jolivet, L., Goffé, B., Monié, P., Truffert-Luxey, C., Patriat, M., Bonneau, M., 1996. Miocene detachment in Crete and exhumation $P–T–t$ paths of high pressure metamorphic rocks. Tectonics 15, 1129–1153.

Jolivet, L., Faccenna, C., d'Agostino, N., Fournier, M., Worrall, D., 1999. The Kinematics of Marginal Basins, examples from the Tyrrhenian, Aegean and Japan Seas. In: Mac Niocaill, C., Ryan, P.D. (Eds.), Continental Tectonics. Geol. Soc. London, vol. 164, pp. 21–53.

Le Pichon, X., Henry, P., Goffé, B., 1997. Uplift of Tibet: from eclogites to granulites—implications for the Andean Plateau and the Variscan Belt. Tectonophysics 273, 57–76.

Malavieille, J., Chemenda, A.I., 1997. Impact of initial geodynamic settings on the structure, ophiolite emplacement and tectonic evolution of collisional belts. Ofioliti 22, 3–13.

Mancktelow, N., 1995. Nonlithostatic pressure during sediment subduction and the development and exhumation of high pressure metamorphic rocks. J. Geophys. Res. 100, 571–583.

Maekawa, H., Shouzui, M., Ishii, T., Fryer, P., Pearce, A.J., 1993. Blueschist metamorphism in an active subduction zone. Nature 364, 520–523.

Maekawa, H., Fryer, P., Ozaki, A., 1995. Incipient blueschist-facies metamorphism in the active subduction zone beneath the Mariana forearc. In: Taylor, B., Natland, J. (Eds.), Active Margins and Marginal Basins of the Western Pacific, vol. 88. American Geophysical Union, Washington, DC, pp. 281–289.

Matte, P., 1998. Continental subduction and exhumation of HP rocks in Paleozoic orogenic belts: Uralides and Variscides. GFF 120, 209–222.

Métivier, F., 1997. Mass transfer between eastern Tien Shan and adjacent basins (central Asia): constraints on regional tectonics and topography. Geophys. J. Int. 128, 1–17.

Molnar, P., Gray, D., 1979. Subduction of continental lithosphere: some constraints and uncertainties. Geology 7, 58–62.

Molnar, P., Lyon-Caen, H., 1989. Fault plane solutions of earthquakes and active tectonics of the Tibetan plateau and its margins. Geophys. J. Int. 99, 123–153.

Petrini, K., Podladchikov, Yu., 2000. Lithospheric pressure–depth relationship in compressive regions of thickened crust. J. Metamorph. Geol. 18, 67–78.

Platt, J.P., 1986. Dynamics of orogenic wedges and the uplift of high-pressure metamorphic rocks. Geol. Soc. Am. Bull. 97, 1037–1053.

Platt, J.P., 1993. Exhumation of high-pressure rocks: a review of concept and processes. Terra Nova 5, 119–133.

Poliakov, A.N.B., Podladchikov, Y., Talbot, C., 1993. Initiation of salt diapirs with frictional overburden: numerical experiments. Tectonophysics 228, 199–210.

Schmid, S.M., Pffifner, O.A., Schönborg, G., Froitzheim, N., Kissling, E., 1997. Integrated cross-sections and tectonic evolution of the Alps along the Eastern Traverse. In: Pffifner, O.A., Lehner, P., Heitzmann, P., Mueller, S., Steck, A. (Eds.), Deep Structures of the Swiss Alps. Birkhäuser, Basel, pp. 289–304.

Selverstone, J., 1988. Evidence for east–west crustal extension in the eastern Alps: implications for the unroofing history of the Tauern window. Tectonics 7, 87–105.

Shi, Y., Wang, C.Y., 1987. Two-dimensional modeling of the $P–T–t$ paths of regional metamorphism in simple overhrust terrains. Geology 15, 1048–1051.

Shreve, R.L., Cloos, M., 1986. Dynamics of sediment subduction, melange formation, and prism accretion. J. Geophys. Res. 91, 10229–10245.

Smith, D.C., 1984. Coesite in clinopyroxene in the Caledonides and its implications for geodynamics. Nature 310, 641–644.

Turner, S., Arnaud, N., Liu, J., Rogers, N., Hawkesworth, C., Harris, N., Kelley, S., Van Calsteren, P., Deng, W., 1996. Post-collision, shoshonitic volcanism on the Tibetan plateau: implications for convective thinning of the lithosphere and the source of Ocean Island Basalts. J. Petrol. 37, 45–71.

Wain, A., 1997. New evidence for coesite in eclogite and gneiss: defining an ultrahigh-pressure province in the Western Gneiss region of Norway. Geology 25, 927–930.

Weinberg, R.F., Podladchikov, Yu., 1994. Diapiric ascent of magmas through power-law crust and mantle. J. Geophys. Res. 99, 9543–9559.